Supplementary information

Piezoelectricity of Strain-induced Overall Water Splitting of $MoS_2/Ni(OH)_2$ Heterostructures

Authors: Kim Tuyen Le[1], Nguyet N. T. Pham[2,7], Yin-Song Liao[1], Ashok Ranjan[1], Hsun-Yen Lin[1,5], Po-Han Chen[1], Hoang Nguyen[3], Ming Yen Lu[1,6], Seung Geol Lee[3,4], and Jyh Ming Wu[1, 6*]

[1]Department of Materials Science and Engineering, National Tsing Hua University
101, Section 2 Kuang Fu Road, Hsinchu 300, Taiwan.

[2]Department of Chemistry, University of Science, Vietnam National University, Ho Chi Minh City, Vietnam.

[3]School of Chemical Engineering, Pusan National University 2, Busandaehak-ro 63 beon-gil, Geumjeong-gu, Busan 46241, Republic of Korea.

[4]Department of Organic Material Science and Engineering, Pusan National University
2, Busandaehak-ro 63 beon-gil, Geumjeong-gu, Busan, 46241, Republic of Korea.

[5]Ph.D. Program in Prospective Functional Materials Industry, National Tsing Hua University
101, Section 2 Kuang Fu Road, Hsinchu 300, Taiwan.

[6]High Entropy Materials Center, National Tsing Hua University
101, Section 2 Kuang Fu Road, Hsinchu 300, Taiwan.

[7]Vietnam National University Ho Chi Minh City, Linh Trung Ward, Thu Duc City, Ho Chi Minh City, 700000, Vietnam

* Prof. J. M. Wu, Email:wujm@mx.nthu.edu.tw

Supplementary information of S1:

Figs. S1a-c shows the SEM images of $Ni(OH)_2/MoS_2$ NFs heterostructures prepared at pH 9 to 11, respectively. The flowerlike morphologies of MoS_2 remained the same after loading $Ni(OH)_2$ NPs and did not show a significant change in the morphology for the different pH values.

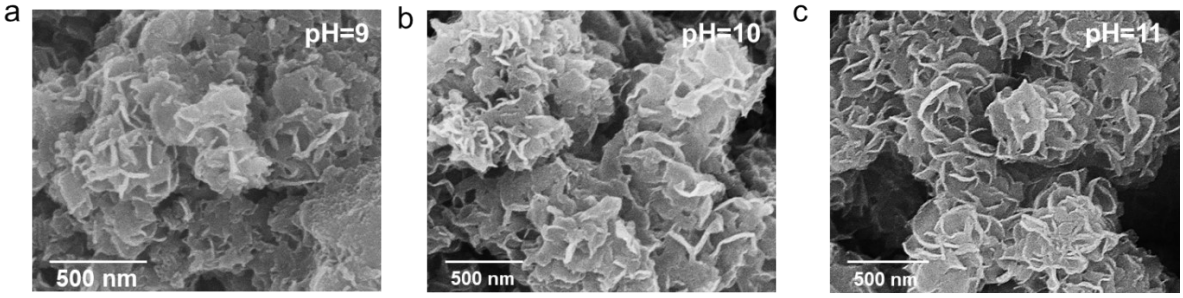

Fig. S1. (a)-(c) The SEM images of $Ni(OH)_2/MoS_2$ NFs heterostructures at pH values from 9, 10, and 11, respectively.

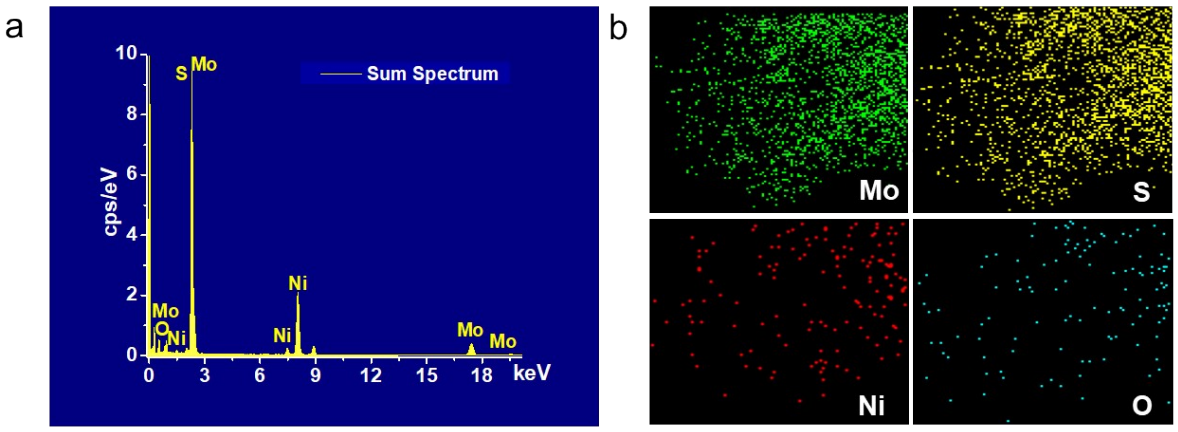

Fig. S2. (a)-(b) The EDS spectrum, mapping of $Ni(OH)_2/MoS_2$ NFs.

Table S1. The corresponding elemental compositions of $Ni(OH)_2/MoS_2$ NFs heterostructure at pH=12 derived from the EDS spectrum.

Element	Atomic %
Mo	32.4
S	58.3
Ni	2.1
O	7.3
Total	100.0

Table S2. Comparisons of HER overpotential (η), Tafel slope, and R_{ct} at OCP of Pt/C 20 wt%, $Ni(OH)_2$, MoS_2 NFs, and heterostructured $Ni(OH)_2/MoS_2$ NFs at different pH values.

Catalyst	Overpotential (mV)- η_{10}	Tafel slope (mV/dec)	R_{ct} (Ω)
$Ni(OH)_2$	465	91.0	-
MoS_2 NFs	250	91.6	92.0
pH=9	221	76.5	52.0
pH=10	182	68.4	24.2
pH=11	182	66.0	14.5
pH=12	155	62.1	7.9
Pt/C 20 wt%	3.2	36.5	-

Table S3. Comparisons of OER overpotential (η), Tafel slope, R_{ct} at 0.8 V (V vs. RHE) of $Ni(OH)_2$, MoS_2 NFs, and heterostructured $Ni(OH)_2/MoS_2$ NFs at different pH values.

Catalyst	Overpotential (mV)- η_{10}	Tafel slope (mV/dec)	R_{ct} (Ω)
$Ni(OH)_2$	373	78.5	-
MoS_2 NFs	570	258.6	100.0
pH=9	340	76.7	76.6
pH=10	336	75.1	44.0
pH=11	335	70.8	12.8
pH=12	328	69.3	10.1

Table S4. Comparisons of HER overpotential (η), Tafel slope (V vs. RHE) of MoS_2 NFs and heterostructured $Ni(OH)_2/MoS_2$ NFs on GS.

Catalyst	Overpotential (mV)-η_{10}	Tafel slope (mV/dec)
Blank GS	424	506.8
MoS_2 NFs	241	221.9
$Ni(OH)_2/MoS_2$ NFs	160	148.9
Pt/C	43	133.6

Supplementary Information of S2:

The E_{2g}^{1} and A_{1g} vibration modes belongs to the 2H MoS_2 at 379.6 cm^{-1} and 405.6 cm^{-1}, respectively. Compared to pristine MoS_2 NFs, the heterostructure with the peaks shifted to a lower wavenumber, and the intensities were weakened due to incorporating $Ni(OH)_2$ onto the MoS_2's surface. Two peaks are positioned at 378.1 cm^{-1} and 403.9 cm^{-1}, which remained the same distance, indicating that after loading $Ni(OH)_2$, MoS_2 NFs remained the single- and few-layered morphology[1].

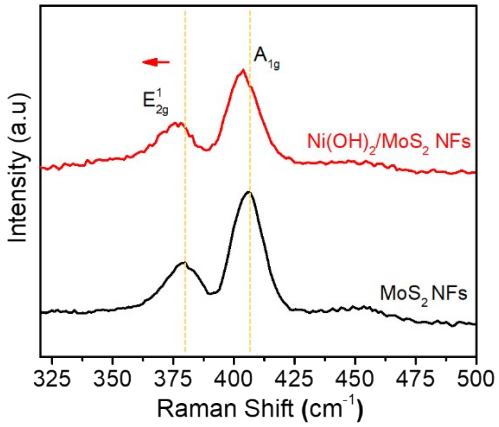

Fig. S3. Raman spectra of pristine MoS_2 NFs and $Ni(OH)_2/MoS_2$ NFs at pH=12

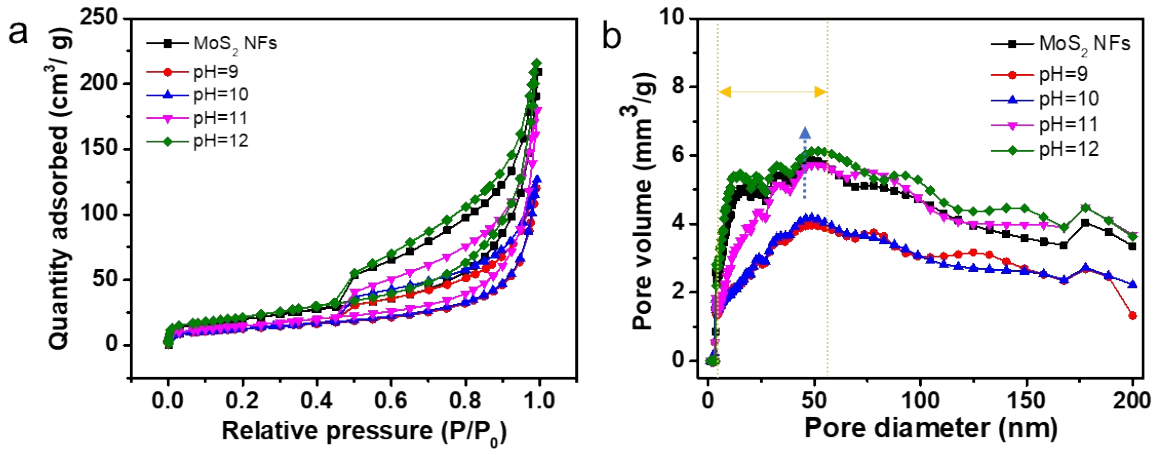

Fig. S4. (a)-(b) The nitrogen adsorption-desorption isotherm; and the analysis of pore volume and pore size of MoS_2 NFs, $Ni(OH)_2/MoS_2$ heterostructures at different pH values, respectively.

Supplementary Information of S3:

As shown in Fig. S5, after the HER stability test, the SEM image (Fig. S5a) demonstrated that the heterostructure morphology remains unchanged. Figs. S5b-e revealed the HRTEM images and SAED pattern, respectively, showing that $Ni(OH)_2$ NPs still exist and were well scattered on MoS_2's surface. The lattice fringe of 0.23 nm is well-agreed with the (101) planes in $Ni(OH)_2$. Fig. 5f shows that the XRD pattern of $Ni(OH)_2/MoS_2$ heterostructures has the same diffraction peaks (compared with Fig. 1d, pH=12, unreacted sample). Besides, XPS spectra have confirmed the coexistence of $Ni(OH)_2$ and MoS_2 NFs. Figs. S5g-h showed that the Mo^{4+} $3d_{3/2}$ and $3d_{5/2}$ peaks are positioned at 232.6 eV and 229.5 eV, respectively, which are assigned to 2H-MoS_2. The peak at 236.0 eV belongs to MoO_3, while the S $2p_{1/2}$ and S $2p_{3/2}$ peaks are located at binding energies of 163.6 eV and 162.4 eV. In addition, Fig. S5i showed that the Ni2p of heterostructures exhibited two peaks, which were positioned at 856.3 eV and 874.0 eV, corresponding to Ni^{2+} for Ni 2p3/2 and Ni 2p1/2,

respectively, attributed to $Ni(OH)_2$ characteristic peaks [1-3]. The results indicated the excellent stability of the heterostructure after the HER stability test.

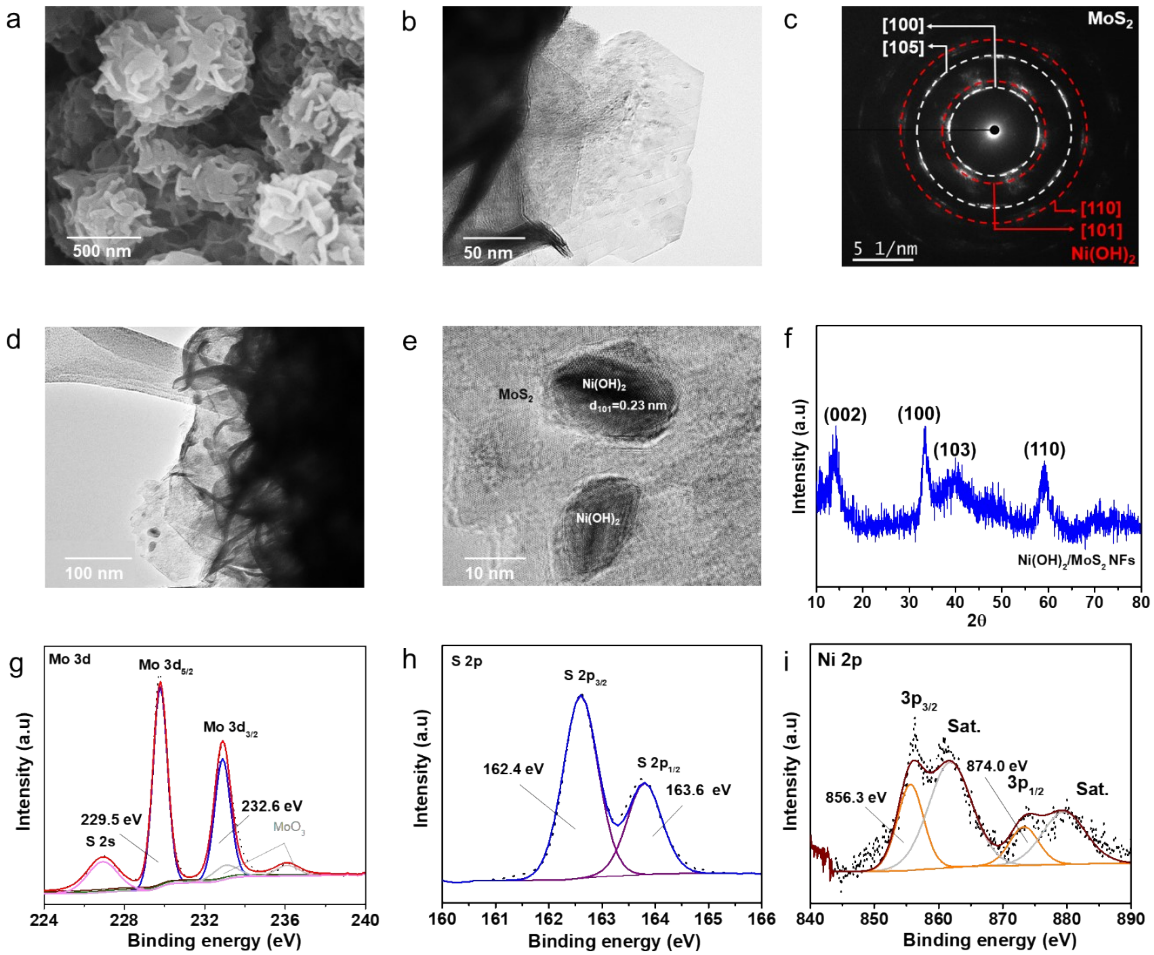

Fig. S5. After the HER stability test, (a) SEM image, (b)-(e) HRTEM image and corresponding SAED pattern, (f) XRD pattern, (g)-(i) the XPS spectra of Mo 3d, S 2p, and Ni 2p of $Ni(OH)_2/MoS_2$ NFs heterostructure at pH=12, respectively.

Supplementary Information of S4:

After the OER stability test, Fig. S6a and S6b show that the SEM image and XRD pattern indicated that the $Ni(OH)_2/MoS_2$'s morphology and crystal structure .remained unchanged (compared with Fig. 1d, pH=12, unreacted sample). The XPS spectra have confirmed the coexistence of $Ni(OH)_2$ and MoS_2 NFs. Figs. S6c-d showed that MoS_2 NFs in heterostructures still maintained mostly the 2H phase. The results were proved by Mo 3d and S2p fitting spectra. The Mo^{4+} $3d_{3/2}$ and $3d_{5/2}$ peaks are positioned at 232.6 eV and 229.5 eV, and the S $2p_{1/2}$ and S $2p_{3/2}$ peaks are located at binding energies of 163.5 eV and 162.3 eV, respectively, corresponding to 2H-MoS_2. Fig. S6e showed the Ni2p of heterostructures exhibited two peaks, which were positioned at 856.3 eV and 874.0 eV, corresponding to Ni^{2+} for Ni 2p3/2 and Ni 2p1/2, respectively, attributed to $Ni(OH)_2$ characteristics peaks[1-3], indicating the excellent stability of the heterostructure after OER stability test.

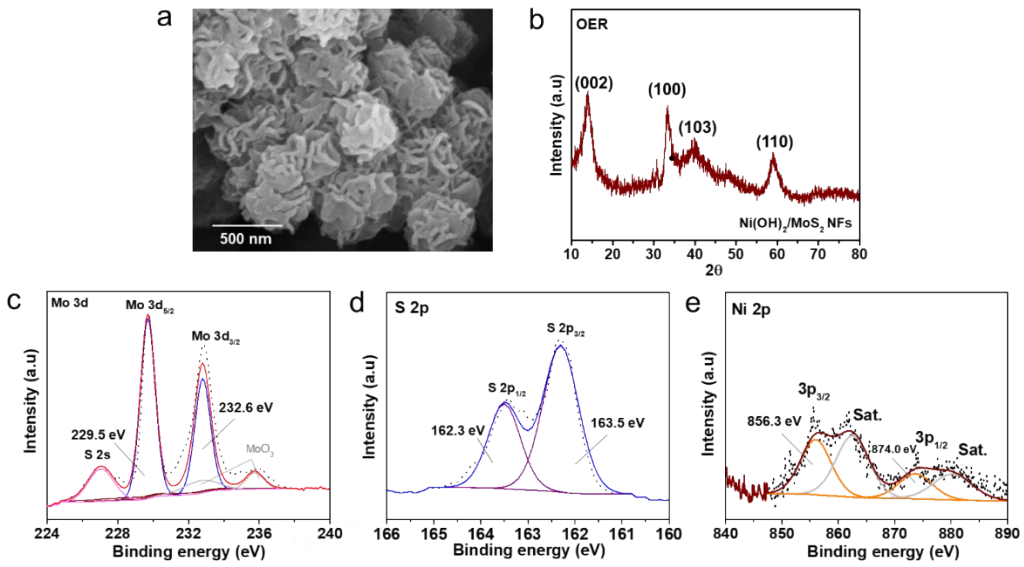

Fig. S6. After the OER stability test, (a) SEM image, (b) XRD pattern, (c)-(e) The XPS spectra of Mo 3d, S 2p, and Ni 2p of $Ni(OH)_2/MoS_2$ heterostructures at pH=12, respectively.

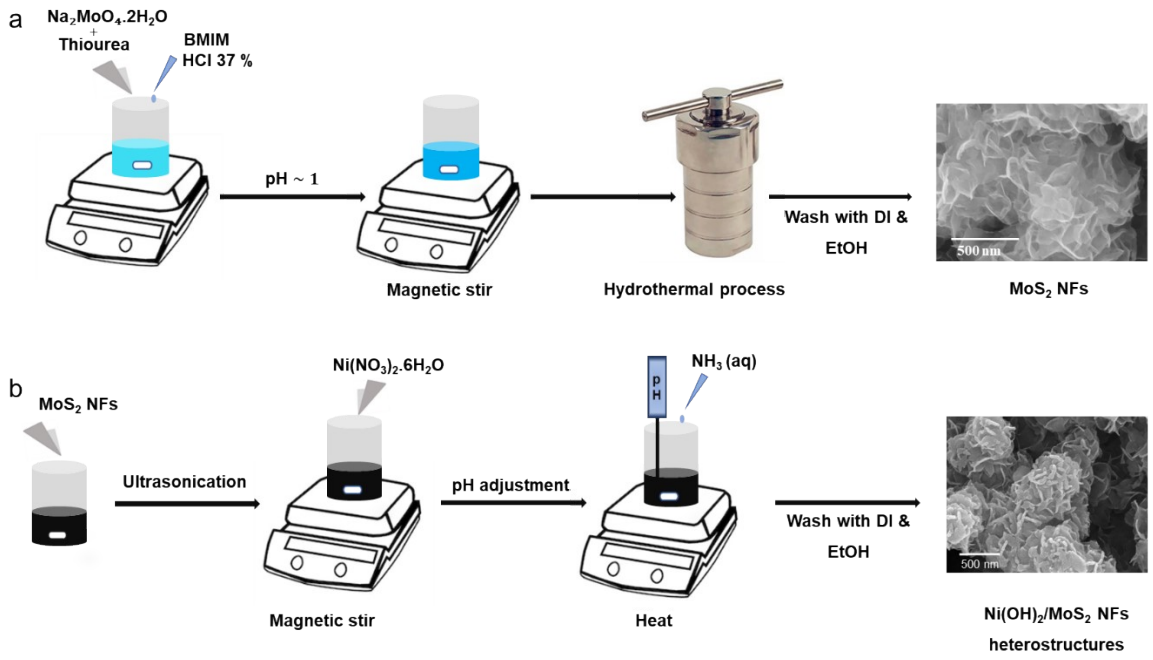

Fig. S7. (a)-(b) Schematic preparation process of MoS_2 NFs, and $Ni(OH)_2/MoS_2$ NFs heterostructures, respectively.

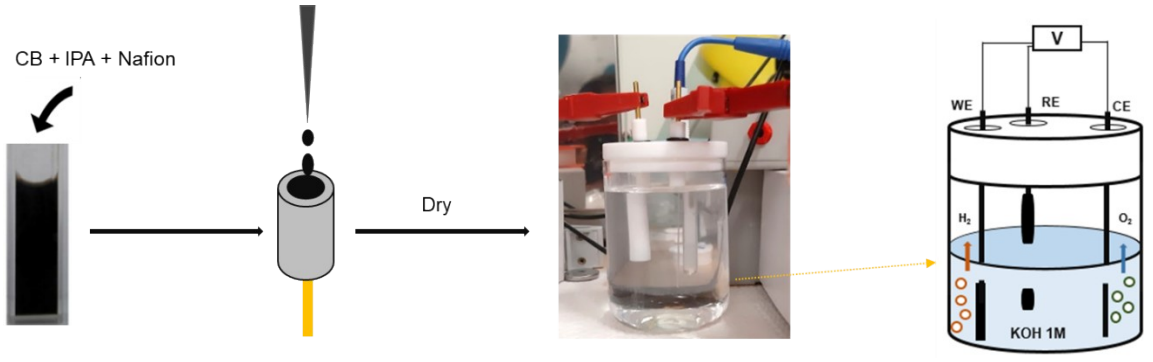

Fig. S8. Illustration of the three-electrode experimental setup.

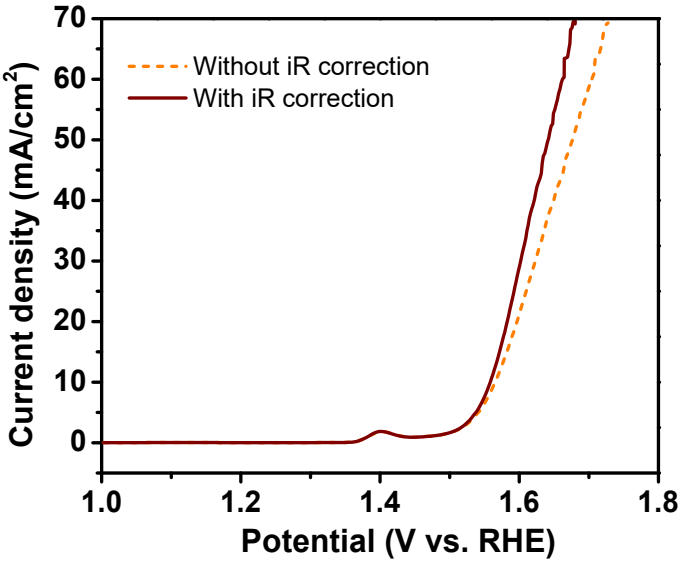

Fig. S9. Comparison with and without iR correction, the iR-corrected LSV was used to calibrate all the measurements to eliminate the resistance of the measuring system.

Reference

1. J. M. Wu, W. E. Chang, Y. T. Chang and C. K. Chang, *Adv. Mater.*, 2016, **28**, 3718–3725.
2. Y. K. Lin, R. S. Chen, T. C. Chou, Y. H. Lee, Y. F. Chen, K. H. Chen and L. C. Chen, *ACS Appl. Mater. Interfaces*, 2016, **8**, 22637−22646.
3. H.-Y. Lin, K. T. Le, P.-H. Chen and J. M. Wu, *Appl. Catal. B*, 2022, **317**, 121717.